PHILOSOPHICAL TRANSACTIONS OF THE ROYAL SOCIETY A MATHEMATICAL, PHYSICAL & ENGINEERING SCIENCES

Stellar Studies in the Balloon Ultraviolet

B. Bates, P. P. D. Carson, P. L. Dufton, C. D. McKeith, A. Boksenberg, B. Kirkham and M. Pettini

Phil. Trans. R. Soc. Lond. A 1975 **279**, 379-390
doi: 10.1098/rsta.1975.0071

Phil. Trans. R. Soc. Lond. A. **279**, 379–390 (1975) [379]
Printed in Great Britain

Stellar studies in the balloon ultraviolet

By B. Bates, P. P. D. Carson, P. L. Dufton, C. D. McKeith
Department of Pure and Applied Physics, The Queen's University of Belfast, Northern Ireland

and A. Boksenberg, B. Kirkham and M. Pettini
Department of Physics and Astronomy, University College, London, W.C. 1

Observations with a spectral resolution of 0.01 nm have been made for several stars in the balloon ultraviolet. For the two coolest stars studied (β Ori and α Lyr) wavelengths of all observed spectral features in the range 273–288 nm are given with an accuracy of approximately ± 0.004 nm. Using these results the velocity field in the atmosphere of β Ori has been investigated and evidence is found for an outward motion in the higher layers and a pulsation-type motion in the deepest layers. The strength of the Mg^+ resonance and subordinate lines near 280 nm for all the stars observed is compared with non-l.t.e. calculations. Good agreement between observation and theory is found for main sequence stars but the stronger lines in the supergiants imply microturbulent velocities > 10 km s^{-1}.

Introduction

The main emphasis in our balloon ultraviolet astronomy programme is a study of the interstellar gas through observations of the resonance lines of Mg^+ (279.55, 280.27 nm) and Mg^0 (285.21 nm). This primary aim is reflected in the choice of programme stars which are predominantly early B-type. Stars studied to date are listed in table 1.

The observations are made from a balloon-borne payload which consists of an altazimuth mounted star pointing platform carrying a high dispersion objective grating spectrograph and an associated fine guidance system. The latter stabilizes the stellar image to a few arc seconds in the direction of dispersion. Stellar spectra are recorded photographically on 103a-O emulsion over the wavelength range 273.0–288.0 nm with a spectral resolution of *ca.* 0.01 nm at a dispersion of *ca.* 0.24 nm mm^{-1} (Boksenberg *et al.* 1972, 1974).

With this dispersion and high resolution in the spectrograms it is relatively straightforward to distinguish between the stellar and interstellar contributions and to determine line strengths for the stellar Mg^+ resonance and subordinate lines (279.08, 279.80 nm). Also, for the cooler stars observed we are able to establish accurate wavelength scales for the stellar features in the rich line spectra and in the case of β Ori these have been used to determine information on atmospheric mass motions.

The data presented here have been obtained from two separate flights of 5.6×10^5 m^3 balloons launched from the NCAR Balloon Flight Station, Palestine, Texas. In the May 1973 flight the payload was recovered from the Gulf of Mexico after some 13 days immersion in seawater. Although the flight emulsion was considerably fogged owing to chemical attack it has been recalibrated and for two stars (λ Sco, α Lyr) it is possible to compare our results with satellite data. The acceptable agreement found from this comparison gives confidence to the emulsion calibration (Boksenberg *et al.* 1975).

TABLE 1. PROGRAMME STARS

flight	star	sp. T.	$v \sin i$† km s^{-1}	number of spectrograms
4 October 1972	γ Cass	B0.5 IVe	—	3
	β Ori	B8 Ia	60	1
	γ Ori	B2 III	50	1
	δ Ori	09.5 II	100	1
	ϵ Ori	B0 Ia	90	1
	ζ Ori	09.5 Ib	120	1
3 May 1973	δ Sco	B0.5 IV	—	1
	λ Sco	B1.5 IV	100	1
	α Lyr	A0 V	—	2
	α Vir	B1 IV	90	3

† Values determined from profiles of Mg^+ subordinate lines assuming other broadening mechanisms to be negligible.

LINE IDENTIFICATIONS FOR β ORI AND α LYR

The strongest features on our spectrograms for all the stars observed are the resonance and the subordinate lines of Mg^+ at approximately 280 nm. In the hotter stars the spectra are otherwise mainly featureless with only the He^0 line at 282.91 nm being clearly seen.

For the cooler stars, β Ori and σ Lyr, many more lines are observed with the spectra of Fe^+ being especially rich. Among the transition metals, lines of Cr^+, V^+ and Ti^+ are also present. As with observations in the visible region, the lines in the supergiant (β Ori) are in general stronger than those in the main sequence star (α Lyr). Other differences between the two spectra can be understood in terms of a higher degree of excitation and ionization in β Ori because of its higher temperature and lower gravity. For example, certain species are observed in the spectra of only one of the stars, Al^+ in β Ori and Mg^0 in α Lyr while in addition the Cr^+ spectrum appears strengthened in the cooler star.

A list of the wavelengths of all the features observed in the spectra of the two stars is given in table 2. Also included are estimates of the strength of these features based on their central depths. In the case of β Ori this scale has been calibrated such that a strength $S = 1$ corresponds to an equivalent width of approximately 5 pm and a strength $S = 8$ corresponds to approximately 40 pm.

The observed stellar wavelengths (λ) given in table 2 were found as follows. From preflight calibration exposures of the emission line spectra of magnesium and iron, a wavelength dependence of the form

$$\lambda = a + bx + cx^2 \tag{1}$$

was deduced, where x corresponds to position on the spectrogram. Using this relation, relative wavelengths accurate to better than ± 0.01 nm were found for the stellar features in the two stars. These wavelengths were sufficiently precise to yield about 15 positive identifications in each spectrum. The laboratory wavelengths of these lines were then used to derive improved values for the constants a, b and c and definitive wavelengths were calculated for all the stellar features. This procedure implicitly assumes that there are no significant differential velocity shifts between the lines used in deriving the dispersion relations. Theoretically we expect this to be the case since most of the lines have equivalent widths between 30 and 40 pm and hence

TABLE 2. STELLAR FEATURES IN THE SPECTRUM OF β ORI AND α LYR

β Ori		α Lyr		identification		
observed λ/nm	strength (S)	observed λ/nm	strength (S)	ion	laboratory λ/nm	multiplet no.
273.699	5	—	—	$\mathrm{Fe^{+}}$	273.697	63
				$\mathrm{Fe^{0}}$	273.696	49
273.954	7	—	—	$\mathrm{Fe^{+}}$	273.955	63
274.138	2	—	—	$\mathrm{Fe^{+}}$	274.140	260
				$\mathrm{Fe^{+}}$	274.132	417
274.321	6	—	—	$\mathrm{Fe^{+}}$	274.320	62
274.676	8	—	—	$\mathrm{Fe^{+}}$	294.649	62
				$\mathrm{Fe^{+}}$	294.698	63
				$\mathrm{Ti^{+}}$	274.670	31
274.933	8	—	—	$\mathrm{Fe^{+}}$	274.932	62
275.101	2	—	—	$\mathrm{Cr^{+}}$	275.104	120
275.327	5	—	—	$\mathrm{Fe^{+}}$	275.329	235
				$\mathrm{Co^{+}}$	275.330	29
275.578	7	275.568	2½	$\mathrm{Fe^{+}}$	275.573	62
				$\mathrm{Cr^{+}}$	275.581	101
		275.782	2	$\mathrm{Fe^{+}}$	275.781	—
				$\mathrm{Cr^{+}}$	275.772	6
276.181	4	—	—	$\mathrm{Fe^{+}}$	276.181	63
				$\mathrm{Fe^{0}}$	276.178	45
276.246	3	276.259	1½	$\mathrm{Fe^{+}}$	276.244	199
				$\mathrm{Fe^{+}}$	276.257	219
				$\mathrm{Cr^{+}}$	276.258	6
276.378	2	276.378	1½	$\mathrm{Fe^{+}}$	276.367	440
				$\mathrm{Fe^{+}}$	276.391	199
				$\mathrm{Ti^{+}}$	296.390	8
		276.489	1⅓	$\mathrm{Ti^{+}}$	276.482	12
				$\mathrm{Cr^{+}}$	276.496	138
				$\mathrm{Fe^{+}}$	276.479	198
276.652	1½	276.655	2	$\mathrm{Cr^{+}}$	276.655	6
276.747	4	276.756	2	$\mathrm{Fe^{+}}$	276.750	235
				$\mathrm{Fe^{+}}$	276.750	273
				$\mathrm{Fe^{0}}$	276.752	46
276.916	4	276.912	1½	$\mathrm{Fe^{+}}$	276.915	200
277.463	2	277.474	3	$\mathrm{Fe^{+}}$	276.469	218
277.792	1½	277.815	1	$\mathrm{Fe^{+}}$	277.789	233
277.926	4	277.928	1½	$\mathrm{Fe^{+}}$	277.930	234
		277.983	1½	$\mathrm{Mg^{0}}$	277.983	6
277.992	1	—	—	$\mathrm{Fe^{+}}$	277.991	348
		278.231	1	$\mathrm{Ti^{+}}$	278.230	28
				$\mathrm{Cr^{+}}$	278.236	183
		278.296	1½	$\mathrm{Mg^{0}}$	278.297	6
278.373	5	278.375	2	$\mathrm{Fe^{+}}$	278.369	234
				$\mathrm{Cr^{+}}$	278.384	252
278.515	2	278.513	2	$\mathrm{Cr^{+}}$	278.510	99
				$\mathrm{Fe^{+}}$	278.521	373
		278.765	2	$\mathrm{Cr^{+}}$	278.761	58
		278.817	1¼	$\mathrm{Fe^{0}}$	278.811	44
				$[\mathrm{Fe^{2+}}$	278.825	120]
		278.990	1	—	—	—

TABLE 2. (*cont.*)

β Ori		α Lyr		identification		
observed λ/nm	strength (S)	observed λ/nm	strength (S)	ion	laboratory λ/nm	multiplet no.
279.081	9	279.078	3	Mg$^+$	279.077	3
279.197	1	—	—	Fe$^+$	279.205	233
279.315	2	—	—	Fe$^+$	279.324	337
279.386	3	279.396	1	Fe$^+$	279.389	198
279.456	1	—	—	—	—	—
P†	—	279.552	6	Mg$^+$	279.552	1
279.798	10	279.797	7	Mg$^+$	279.799	3
279.924	2	—	—	Fe$^+$	279.929	233
280.066	1	—	—	Ti$^+$	280.065	28
		280.085	4	Cr$^+$	280.077	182
280.174	1½	—	—	—	—	—
P	—	280.270	7	Mg$^+$	280.270	1
280.498	1	—	—	Ti$^+$	280.500	25
				Fe$^+$	280.501	438
280.553	1¼	280.548	¾	V$^+$	280.554	120
		280.712	1	Fe$^+$	280.717	281
				Fe$^+$	280.717	295
		280.839	1	{Mn^0	280.839	13}
		280.984	1	Fe$^+$	280.980	380
		281.138	1½	Cr$^+$	281.145	66
				Cr$^+$	281.145	98
		281.215	1	V$^+$	281.216	143
281.357	2	281.359	1¼	Fe$^+$	281.361	198
281.621	2	—	—	Al$^+$	281.619	7
281.706	1	—	—	Fe$^+$	281.711	380
				Cr$^+$	281.700	307
		282.124	1	{V$^+$	282.112	86}
282.221	2	282.226	2	{Sc$^+$	282.217	5}
282.328	2	282.328	2	Fe^0	282.328	44
		282.581	1½	Fe$^+$	282.575	195
				V$^+$	282.586	221
282.871	2	282.866	2	Fe$^+$	282.862	231
				Fe$^+$	282.868	255
		283.045	1	Cr$^+$	283.046	82
				V$^+$	283.040	155
		283.153	1½	Fe$^+$	283.156	217
		283.237	1	Fe$^+$	283.227	347
				Cr$^+$	283.245	195
				Fe^0	283.244	44
		283.322	1	—	—	—
283.360	1	—	—	—	—	—
283.567	5	—	—	Fe$^+$	283.572	216
283.651	1	—	—	Fe$^+$	283.651	294
				V$^+$	283.653	61
283.966	1	—	—	Ti$^+$	283.970	25
		284.024	1	{Fe$^+$	284.034	195}

† Denotes blending from interstellar line.

TABLE 2. (*cont.*)

β Ori		α Lyr		identification		
observed λ/nm	strength (S)	observed λ/nm	strength (S)	ion	laboratory λ/nm	multiplet no.
284.050	5	284.063	3½	Fe$^+$	284.064	217
				Cr$^+$	284.043	115
				V$^+$	284.059	36
284.199	1	284.186	1½	Ti$^+$	284.191	7
				V$^+$	284.204	35
				Fe$^+$	284.208	196
		284.230	1½	Cr$^+$	284.232	228
284.328	4	284.326	4	Cr$^+$	284.324	5
				Fe$^+$	284.332	231
284.551	3	284.550	2	Fe$^+$	284.545	399
		284.719	1½	Fe$^+$	284.721	197
284.804	4	284.804	1½	Fe$^+$	284.805	196
284.964	4	284.979	3½	Fe$^+$	284.960	196
				Cr$^+$	284.983	5
		285.138	2	Cr$^+$	285.135	82
				Fe$^+$	285.143	195
P		285.208	4	Mg^0	285.212	1
		285.316	2	Fe$^+$	285.312	294
				Cr$^+$	285.318	84
				Fe$^+$	285.320	197
		285.415	1½	Cr$^+$	285.432	161
		285.558	1½	Ti$^+$	285.549	24
				Cr$^+$	285.567	5
				Fe$^+$	285.567	196
		285.627	1	Ti$^+$	285.624	24
				Cr$^+$	285.632	81
		285.676	1	Cr$^+$	285.677	11
		285.737	1	Cr$^+$	285.740	11
				Fe$^+$	285.742	195
		285.844	2	Ti$^+$	285.840	6
				Fe$^+$	285.851	354
		285.873	4	Fe$^+$	285.864	399
		286.103	3	Fe$^+$	286.119	61
		286.244	3	Ti$^+$	286.234	16
				Cr$^+$	286.257	5
		286.359	1	—	—	—
		286.512	4	Cr$^+$	286.510	5
		286.665	2	Cr$^+$	286.672	5
				Fe^0	286.662	43
		286.706	1	Cr$^+$	286.709	11
		286.760	2	Cr$^+$	286.765	5
		286.885	1	Fe$^+$	286.887	61
		287.042	3	Cr$^+$	287.043	11
		287.107	1½	Fe$^+$	287.106	195
				Fe$^+$	287.113	230
		287.169	1	Mn$^+$	287.168	109
		287.239	2½	Fe$^+$	287.238	230
				Fe$^+$	287.233	43
		287.341	5	Fe$^+$	287.340	279
				Cr$^+$	287.346	5
		287.372	2	—	—	—

are presumably formed at similar continuum optical depths. In addition, differential velocity shifts would increase values for the average wavelength residuals while the observed values of ± 0.0032 nm for β Ori and ± 0.0035 nm for α Lyr are consistent with errors in measurement. We therefore conclude that for well observed unblended lines, the stellar wavelengths given in table 2 are accurate to within ± 0.004 nm.

This high precision in the wavelength measurements permits in most cases a positive identification of the stellar features. These identifications are listed in the final columns of table 2, where marginal contributors to any blend are enclosed in brackets. The multiplet numbers and laboratory wavelengths are from Moore (1962).

The velocity field in the atmosphere of β Ori

In general atmospheres of Ia-type supergiants exhibit mass motions. Usually this is an expansion, in which the velocity field is a function of both optical depth and time (see; for example, Hutchings 1970). For β Ori Stecher (1968) reports large expansional velocity shifts for lines in the rocket ultraviolet while Chentsov & Snezhko (1971: CS) have found that the Hβ line is blue shifted by 10–20 km s^{-1} relative to H_{20}. These latter authors also investigated the radial velocities of the visual metal line spectra in this star. For lines formed deep in the atmosphere (continuum optical depth 10^{-1} to 1) they observed small variations in radial velocity with time and suggest that on occasions the velocity field in this region corresponds to an inward motion. For the stronger lines formed higher in the atmosphere, radial velocity variations were also observed but here the flow of material was always outwards. CS propose a model for β Ori in which only the outer layers expand continuously while the deeper layers may be involved in pulsation-type motions.

We have investigated the line shifts for the Fe^+ lines listed in table 2 and determined their dependence on line strength. In order to relate the strength of a line to a depth of formation, a model for the atmosphere of β Ori is needed. A simple l.t.e. model atmosphere has been used, in which the temperature–optical depth structure is due to Klinglesmith (1971). Our model has an effective temperature (T_{eff}) of 14000 K and a logarithmic gravity (lg g) of 1.85; these parameters were deduced from fitting theoretical calculations for the Balmer discontinuity and the equivalent width of the Hγ line to the observational data of Schild *et al.* (1971) and Underhill (1970*a*) respectively. Details of the computational procedure can be found in Dufton (1972), the only significant change being in the calculation of the strength of Hγ where the recent Stark broadening formulation of Vidal, Cooper & Smith (1973) was used. A depth independent microturbulence has been assumed and its magnitude was estimated in two ways. First, for a magnesium to hydrogen abundance in β Ori similar to that in other B-type stars (Mihalas 1972), the equivalent widths of the Mg^+ subordinate lines indicate a microturbulent velocity of approximately 15 km s^{-1}. Secondly an observational curve of growth for Fe^+ lines with excitation potentials around 3.2 eV was compatible with theoretical curves having microturbulent velocities between 10 and 20 km s^{-1}. A microturbulence of 15 km s^{-1} was therefore adopted for this star. This value may be compared with the 22 km s^{-1} found by van Helden (1972) for the B5Ia star o^2 CMa. For an extreme supergiant such as β Ori, the choice of atmospheric parameters must be uncertain but fortunately test calculations show that the results presented below are very insensitive to the details of the model.

Using this model atmosphere we have calculated the depth of formation of the Fe^+ line cores for different values of equivalent width. From these results and the observed relationship between radial velocity and line strength it is possible to deduce the radial velocity at different depths in the atmosphere, and the results are shown in figure 1. We note that for the layers in which the Fe$^+$ lines are formed, the range in the velocity shifts is considerably smaller than the Gaussian half-widths of these lines and hence the use of a static atmosphere for calculating equivalent widths should be valid.

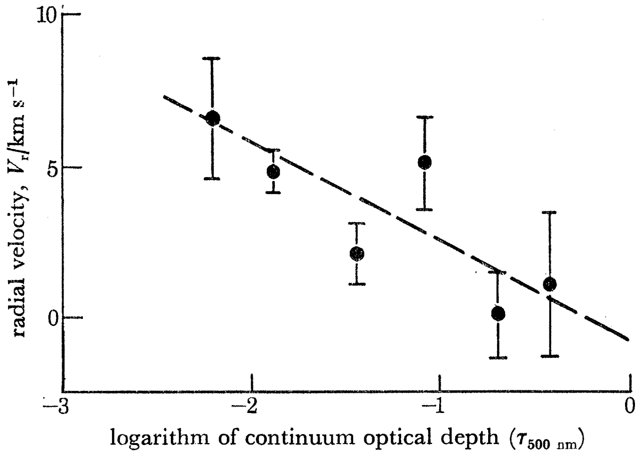

FIGURE 1. Radial velocities for the Fe$^+$ lines in β Ori. Mean values and standard deviations are given for groups of lines formed at similar optical depths ($\tau_{500\ \mathrm{nm}}$ is the continuum optical depth at 500 nm for which the line centre optical depth = 1). Also included at lg $\tau_{500\ \mathrm{nm}} \approx -2.2$ is a velocity for the Mg$^+$ subordinate lines. Here the error shown follows from our estimate of the accuracy of the wavelength measurements. The radial velocity scale has been normalized to 0 km s^{-1} at $\tau_{500\ \mathrm{nm}} = 1$.

The strong Mg$^+$ resonance lines provide information on the radial velocity field for values of $\tau_{500\,\mathrm{nm}} < 7\times10^{-3}$. A visual examination of the microdensitometer traces indicates that the resonance lines are blue shifted. However, it is difficult to make a direct estimate of the magnitude of this shift because of blending with the strong interstellar lines. The method we have used is to compare the observed spectrum in the region of the resonance lines with synthesized spectra which as well as the lines of Mg$^+$ include weaker features due to Fe$^+$ and Ti$^+$. The calculations use the model atmosphere described above and also include the velocity field for $\tau_{500\,\mathrm{nm}} > 7\times10^{-3}$ shown in figure 1. For higher regions in the atmosphere ($\tau_{500\,\mathrm{nm}} < 7\times10^{-3}$) the velocity field is varied to produce a best fit between the theoretical and observational spectra. The profiles of the Mg$^+$ subordinate lines indicate an equatorial rotational velocity of 60 km s^{-1} and the synthesized spectra have been convoluted with a broadening function with this width.

Figure 2 shows two examples of the comparison between observed and synthesized spectra. For the case of zero velocity shift for optical depths $<7\times10^{-3}$ the calculated spectrum gives only a poor fit to experimental data especially in the short wavelength sides of the resonance lines. Also shown is the synthesized spectrum for a velocity field having a relation

$$V_r = 7 - 40\ \mathrm{lg}\ (7\times10^{-3}/\tau_{500\,\mathrm{nm}}) \qquad (2)$$

for $\tau_{500\,\mathrm{nm}} < 7\times10^{-3}$. In the spectral region of the Mg$^+$ resonance lines the agreement with the observed spectra is considerably improved and for the region of formation of the line cores ($\tau_{500\,\mathrm{nm}} \approx 5\times10^{-4}$) the radial velocity is -40 km s^{-1}. Other radial velocity distributions will also give a good agreement with observation but they all have the property of indicating a velocity shift of approximately -40 km s^{-1} in the region of formation of the cores of the lines. As expected the different velocity fields for $\tau_{500\,\mathrm{nm}} < 7\times10^{-3}$ have little influence on other spectral features which are formed at deeper levels in the atmosphere.

These results suggest the existence of two distinct regions in the atmosphere of β Ori. In the outermost layers there is an expansion of the order of 40 km s^{-1} relative to the region in which the continuum is formed. This result is compatible with those of previous studies of this star.

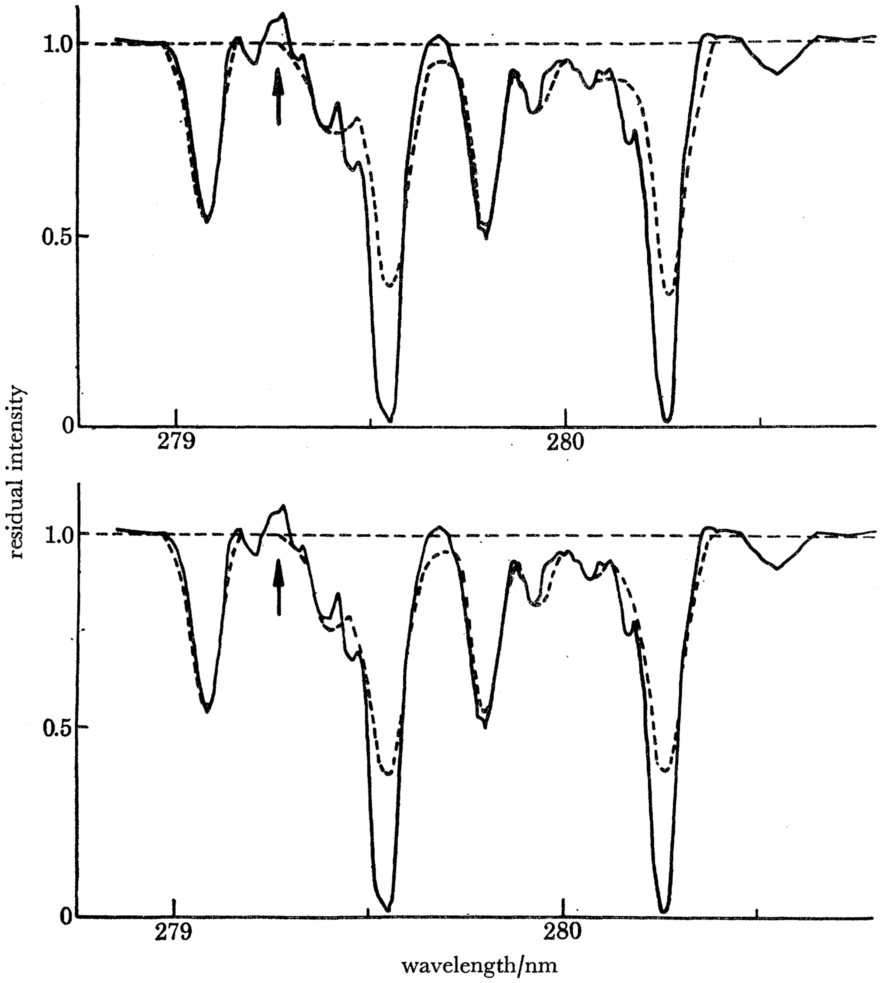

FIGURE 2. Comparison of observed (——) and synthesized spectra (— —) for β Ori in the region of the Mg$^+$ resonance lines. The upper theoretical curve corresponds to a zero radial velocity shift for optical depths $\tau_{500\ \mathrm{nm}} < 7\times10^{-3}$ and the lower curve to the velocity field given in equation (2).

For deeper levels in the atmosphere however, the results shown in figure 1 indicate an inward flow of material relative to the continuum region. This situation cannot be stable since it leads to a depletion of matter near the boundary of the two regions. Although the velocity shifts are small and may be time dependent, the inward motion suggested here for intermediate optical depths does give some support to the suggestion by Chentsov and Snezhko of a pulsation-type motion occurring in the atmosphere of β Ori.

Other studies of velocity fields in early-type supergiants include Groth (1972), who has examined in detail time dependent differential line displacements in α Cyg (A2Ia) in terms of models which include depth dependent microturbulent and radial velocity fields, and Aydin (1972), who has found evidence for an inward motion in the atmosphere of one star, HD21389 (A0Ia). For this star the variation of radial velocity with depth was deduced from observations of the cores of the Balmer line series. This study will presumbably refer to smaller optical depths than for our investigation of the Fe^+ line spectrum, but it too provides additional evidence for the existence of pulsation-type motions in early-type supergiants.

COMPARISON OF THE Mg^+ RESONANCE AND SUBORDINATE LINE STRENGTHS WITH MODEL ATMOSPHERE CALCULATIONS

Underhill (1970*b*) and Mihalas (1972) have pointed out that the spectral lines of Mg^+ are sensitive to non-l.t.e. effects. Using both l.t.e. and non-l.t.e. model atmosphere calculations Mihalas has predicted the strength of the Mg^+ lines arising from the 3s–3p (279.55, 280.27 nm); 3p–3d (279.08, 279.80 nm); 3d–4f (448.1 nm) transitions. Comparing his data with observations for the 448.1 nm doublet he finds that the observed equivalent widths fit a non-l.t.e. model with approximately solar magnesium abundance and a microturbulent velocity of 4 km s^{-1} over the entire range of spectral type from B5 to O6. This is in contrast to the l.t.e. calculations where agreement is poor for the earlier spectral types. Mihalas shows that the non-l.t.e. calculations yield stronger lines than l.t.e., the difference in line strength increasing with effective temperature. He emphasizes that large systematic errors are likely to result from abundance determinations using l.t.e. models.

It is important to extend this study to the ultraviolet resonance and subordinate lines since these have larger equivalent widths and are more sensitive to non-l.t.e. effects than the visible doublet. Lamers, van der Hucht, Snijders & Sakhibulin (1973) have reported on an investigation of the total equivalent width (resonance plus subordinate lines) in the spectra of over 30 stars which were observed from the TD-1A satellite. They find that observations for luminosity classes II–V agree with non-l.t.e. models for spectral types later than B3 but in early B-stars the observed lines are too strong. They also report that in general, B-type supergiants have stronger lines than main sequence stars of the same spectral type.

It is necessary to correct the observed total equivalent width of the Mg^+ lines for the interstellar contribution arising from the resonance lines. Lamers *et al.* point out that our results for interstellar equivalent widths (Boksenberg *et al.* 1972, 1973) indicate that their interstellar corrections may have been underestimated, and this may account for a significant part of the discrepancy between observation and theory for the earlier spectral types (H. J. Lamers 1972, personal communication).

With the higher resolution of our spectra it is possible to make a more accurate determination of the interstellar contribution, and in addition, we are able to study the equivalent widths of the individual lines as a function of spectral type. The subordinate lines are relatively unblended and there is therefore no great difficulty in measuring profiles and equivalent widths. Since the main broadening mechanisms for these lines are rotational and macroturbulent velocity fields, the profiles of the stellar resonance lines should be similar to those of the subordinate lines. We have therefore estimated the equivalent widths of the resonance lines by fitting the observations with profiles of different strength whose shape is taken from the subordinate lines. This fitting procedure occurs in the wings of the lines where the narrow interstellar components are negligible. An example is shown in figure 3 for the 279.553 nm Mg^+ resonance line in

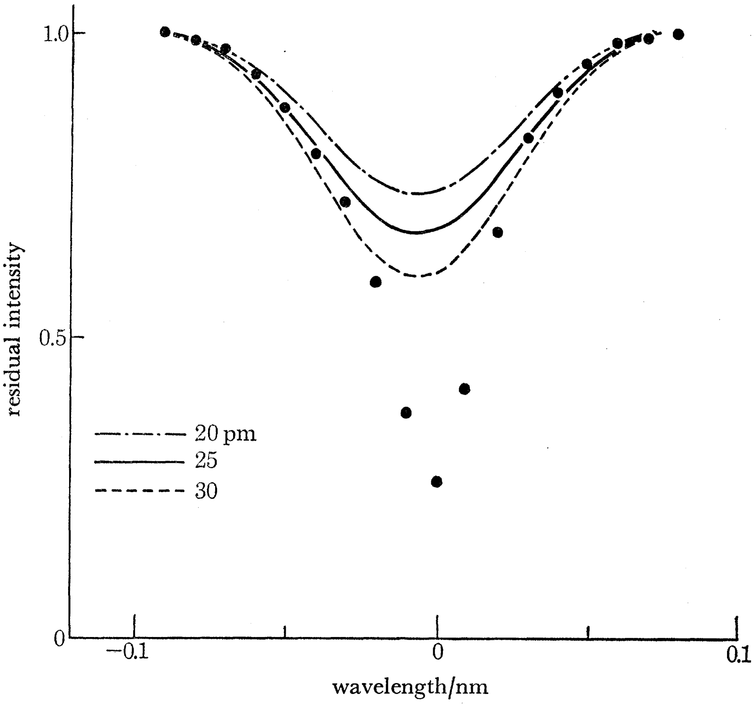

FIGURE 3. Examples of the procedure for estimating the strength of the stellar Mg^+ resonance lines. Observational points are for the 279.553 nm line in γ Ori. Line profiles having the same shape as the subordinate lines in this star are shown for different equivalent widths. The curve for 25 pm gives the best fit in the stellar line wings.

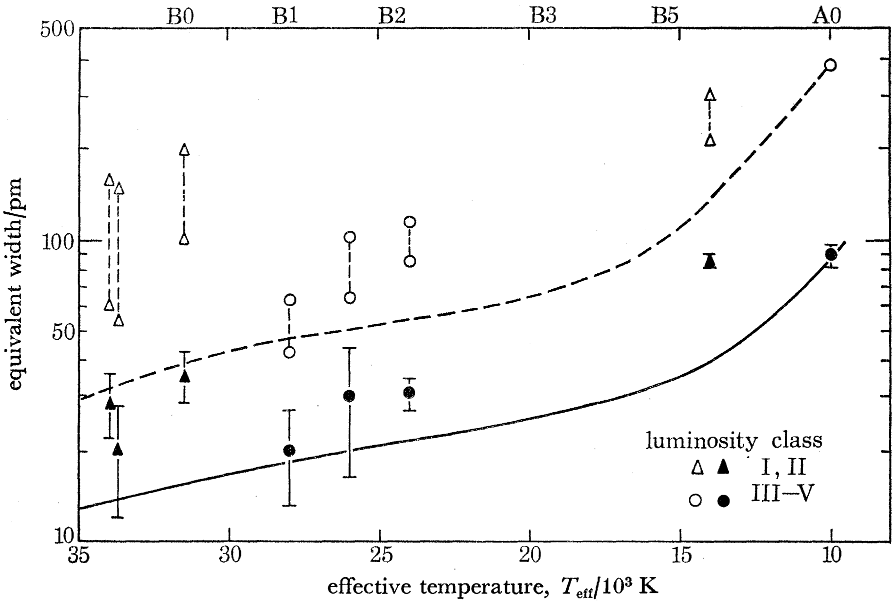

FIGURE 4. Comparison of the Mg^+ line strengths with model atmosphere calculations. The open symbols give the total equivalent width of the resonance plus subordinate lines. For each pair, the upper value includes the interstellar contribution. Solid symbols refer to the subordinate lines alone. The curves refer to the non l.t.e. calculations of Mihalas (1972) for the total (– – –) and subordinate line (——) equivalent widths.

γ Ori. The profile corresponding to an equivalent width of 25 pm gives a good fit in the line wings but the 20 and 30 pm curves are too weak and too strong.

Figure 4 provides a summary of observed equivalent widths as a function of spectral type. One set of values for the total equivalent width includes the interstellar contribution. It is evident that the interstellar corrections shown for the early B-type stars are very large and for the more distant stars studied, the stellar contribution to the equivalent width is only about 30–40 % of the total observed value. The subordinate lines require no correction for interstellar absorption and the line strengths may be compared directly with computed data. Error estimates shown for these lines are based on the quality of the spectrograms and also on the internal consistency of the equivalent width measurements.

Non-l.t.e. calculations due to Mihalas (1972) for the total and the subordinate line equivalent widths are also shown in figure 4. All calculations refer to models with $\lg g = 4$, a microturbulent velocity of 4 km s^{-1} and a Mg/H ratio of 2×10^{-5} by number. For a model atom including levels of Mg^{+}, Mg^{2+} and Mg^{3+}, the equations of statistical equilibrium were solved to yield level populations and hence equivalent widths for selected transitions. The high gravity will make these calculations more applicable to the main sequence stars. In general the agreement between theory and observation is good for these stars even up to the earliest spectral types; γ Ori (B2III) has observed equivalent widths larger than the theoretical values but the $\lg g$ for this star may well be less than 4. As Mihalas points out for the 448.1 nm line, a slightly higher magnesium abundance would improve the fit to observation.

For the supergiant stars the line strengths are systematically larger than for the main sequence stars in agreement with Lamers *et al.* (1973). The calculations shown are not appropriate to these stars and we have computed Mg^{+} line strengths for models due to Mihalas (1973) with effective temperatures of 30000 K, $\lg g = 3$ and 4 and a zero microturbulence. The methods and atomic constants used are very similar to those of Mihalas (1972) and the computer code was adapted from one published by Auer, Heasley & Milkey (1973). The results for the model with $\lg g = 4$ are in excellent agreement with the corresponding results of Mihalas. For the $\lg g = 3$ model, the equivalent widths of both the subordinate and resonance lines are decreased by 40–50 % compared with the main sequence model. Thus the observed increase in strength of these lines in the supergiants near B0 is not due to purely non-l.t.e. effects.

A high microturbulence in supergiant atmospheres is well established from l.t.e. studies. We have therefore calculated line strengths for a model with the same effective temperature and gravity but with a microturbulent velocity of 10 km s^{-1}. Although this leads to an increase in the calculated equivalent widths, they remain smaller than observation by a factor of 2–3. Therefore for supergiants near B0 agreement between non-l.t.e. calculations and observation will require microturbulent velocities higher than 10 km s^{-1} together with possibly an increase in the magnesium abundance.

The results presented are from the preliminary stages of our programme and it is hoped to extend the observational data from further planned balloon flights. In the theoretical investigation calculations will be made of line strengths for a wider range of atmospheric parameters and Mg abundance. Also, we intend to use a more quantitative parameter such as the Balmer discontinuity or the Strömgren c_1 colour to improve our estimates of effective temperature. This is necessary for detailed studies since in figure 4, the T_{eff}-spectral type relation was taken from Mihalas (1972) and there is an uncertainty in this scale by, for example, ± 2000 K for a B0 star. In addition, this temperature scale was derived for main sequence stars and hence will not be appropriate for supergiant stars which are expected to have systematically lower temperatures.

Considerable support and encouragement in this balloon programme has come from Sir Harrie Massey, Sec.R.S., Professor D. J. Bradley and Professor H. B. Gilbody. We thank our colleagues at Belfast and London for their effort in the joint project, especially S. McC. Noble, W. A. Towlson, T. E. Venis and D. Wilkinson, and the personnel at N.C.A.R. Palestine for launch and recovery operations. Financial support from the Science Research Council is gratefully acknowledged.

REFERENCES (Bates *et al.*)

Auer, L. H., Heasley, J. N. & Milkey, R. W. 1972 *Contr. Kitt Peak Nat. Observ.* no. 555.
Aydin, C. 1972 *Astron. & Astrophys.* **19**, 369.
Boksenberg, A., Kirkham, B., Towlson, W. A., Venis, T. E., Bates, B., Courts, G. R. & Carson, P. P. D. 1972 *Nature Phys. Sci.* **240**, 127.
Boksenberg, A., Kirkham, B., Towlson, W. A., Venis, T. E., Bates, B., Carson, P. P. D. & Courts, G. R. 1974 *Space Res.* **14**, 553.
Boksenberg, A., Kirkham, B., Michelson, E., Pettini, M., Bates, B., Carson, P. P. D., Courts, G. R., Dufton, P. L. & McKeith, C. D. 1975 *Phil. Trans. R. Soc. Lond. A.* **279**, 303 (this volume).
Chentsov, E. L. & Snezhko, L. I. 1972 *Colloquium on supergiant stars,* Trieste Observatory, (ed. M. Hack), p. 15.
Dufton, P. L. 1972 *Astron. & Astrophys.* **16**, 301.
Groth, H. G. 1972 *Astron. & Astrophys.* **21**, 337.
Hutchings, J. B. 1970 *Mon. Not. R. astr. Soc.* **147**, 161.
Klinglesmith, D. A. 1971 *NASA Special Publication* SP3065.
Lamers, H. J., van der Hucht, K. A., Snijders, M. A. J. & Sakhibulin, N. 1973 *Astron. & Astrophys.* **25**, 105.
Mihalas, D. 1972 *Astrophys. J.* **177**, 115.
Mihalas, D. 1973 *NCAR Technical Note* STR-76.
Moore, C. E. 1962 *An ultraviolet multiplet table*, National Bureau of Standards, Washington.
Schild, R. E., Peterson, D. M. & Oke, J. B. 1971 *Astrophys. J.* **160**, 95.
Stecher, T. P. 1968 *Bull. astr. Insts. Csl.* **19**, 279.
Underhill, A. B. 1970*a* *Astron. & Astrophys.* **6**, 114.
Underhill, A. B. 1970*b* *Spectral line formation in steady state extended atmospheres* (eds H. G. Groth and P. Willman) p. 3. National Bureau of Standards, Washington.
Van Helden, R. 1972 *Astron. & Astrophys.* **19**, 388.
Vidal, C. R., Cooper, J. & Smith, E. W. 1973 *Astrophys. J. Suppl.* **25**, 37.